Kinetics and Mechanism of Degradation and Mineralization of Acetone in Dilute Aqueous Solution Sensitized by the UV Photolysis of Hydrogen Peroxide

ARTICLE *in* ENVIRONMENTAL SCIENCE & TECHNOLOGY · JULY 1996

Impact Factor: 5.33 · DOI: 10.1021/es950866i

3 AUTHORS, INCLUDING:

James R Bolton
University of Alberta
315 PUBLICATIONS **9,533** CITATIONS

SEE PROFILE

Environ. Sci. Technol. **1996**, *30,* 2382−2390

Kinetics and Mechanism of the Degradation and Mineralization of Acetone in Dilute Aqueous Solution Sensitized by the UV Photolysis of Hydrogen Peroxide

MIHAELA I. STEFAN,
AITKEN R. HOY, AND
JAMES R. BOLTON*

Photochemistry Unit, Department of Chemistry, The University of Western Ontario, London, Ontario, Canada N6A 5B7

Acetone is a significant pollutant in contaminated groundwaters and industrial effluents. It can be treated by the UV/H_2O_2 process but only slowly. This study aims to understand the degradation mechanism and hence the reasons for slow treatment. The degradation of acetone was carried out in a UV reactor in the presence of ~16 mM H_2O_2 such that most of the UV was absorbed by H_2O_2. The decay of acetone was followed by gas chromatography, and the generation of intermediates (identified as acetic, formic, and oxalic acids) was followed by ion chromatography. Measurement of the total organic carbon indicated a complete carbon balance throughout the reaction ending in mineralization. A kinetic model, based on an assumed mechanism, was developed that generated a profile of reactants and intermediates in agreement with the experimental data, including the pH profile. The initial concentrations of acetone and hydrogen peroxide strongly affect the initial rate of acetone degradation, but no pH effect was observed in the range of 2−7. It is concluded that acetone treats slowly because intermediates build up to such a concentration that they compete significantly for hydroxyl radicals and also because the mechanism appears to involve some degree of acetone recycling.

Introduction

Photochemical methods for removing toxic organic pollutants, which have been discharged into the aquatic environment, are being applied in an ever increasing number of cases. UV light or sunlight has been used in the direct photodegradation of contaminants in aqueous environments, but neither is considered an efficient method for the destruction of the majority of the target pollutants because the success of direct photolysis is highly dependent on the photoreactivity of the specific organic compounds.

* Corresponding author: e-mail address: jbolton@julian.uwo.ca; telephone: 519-661-2170; fax: 519-661-3022.

Since the late 1960s, many studies have indicated that the UV/H_2O_2 process is able to oxidize a wide variety of organic pollutants in aqueous solutions. For example, Omura and Matsuura (*1*) used this system for the treatment of some phenols, while Ogata *et al.* (*2*) removed biologically refractory nonionic surfactants from wastewaters.

During the past decade, photoinduced oxidation methods using UV light and added H_2O_2 have been improved markedly for the remediation of groundwater and industrial wastestreams (*3*). These UV-based advanced oxidation technologies are well-established industrially and have been installed at over 200 sites (primarily in North America) for the treatment of contaminated waters. The major advantages of these technologies are as follows: (a) high rates of pollutant oxidation (most organic contaminants are eventually completely mineralized to harmless chemicals, such as CO_2, H_2O, and halide ions); (b) large range of applicability regardless of water quality; (c) convenient dimensions of the equipment (*3, 4*).

Some concerns, such as high operating costs (in some cases) and special safety requirements due to the use of very reactive chemicals (e.g., ozone, hydrogen peroxide) and high-energy sources (UV lamps) have been raised regarding these methods. Nevertheless, these concerns can be largely removed in properly designed industrial systems.

Many studies have been carried out on the UV/H_2O_2-induced destruction of aromatic pollutants, such as benzene, toluene, chlorobenzene, phenol, 2-chlorophenol, 2,4-dichlorophenol, 2,4,6-trichlorophenol, dimethyl phthalate (*5, 6*), non-halogenated aliphatics [e.g., methanol (*7*)], and halogenated aliphatics [e.g., trichloroethylene (TCE), perchloroethylene (PCE) (*8, 9*), and 1,2-dibromo-3-chloropropane (*10*)].

Generally, the effectiveness of homogeneous light-driven oxidation processes is associated with very reactive species, such as hydroxyl (·OH) radicals, which are generated in the reaction mixture by the direct photolysis of an added component (e.g., hydrogen peroxide) under UV irradiation. For example

$$H_2O_2 + h\nu \rightarrow 2{\cdot}OH \qquad (1)$$

The hydroxyl radicals attack organic compounds relatively non-selectively with rate constants ranging from 10^6 to 10^{10} M^{-1} s^{-1}, oxidizing them by hydrogen atom abstraction or by addition to double bonds.

Acetone is among the organic compounds identified as hazardous air and industrial wastewater pollutants. Acetone photochemistry has been studied by many workers (*11*−*17*) in the pure liquid as well in the gas phase for over 50 years, but only a few reports on its decomposition by UV light irradiation in dilute aqueous solution exist (*18*−*20*). Acetone is not only a weak absorber but also degrades very slowly by direct photolysis [quantum yield of 0.061 at 270 ± 2.5 nm (*19*)]. The principal products were observed to be methane, acetic acid, formic acid, and ethane depending on the level of oxygen concentration in the studied system. There have been no previous studies of acetone degradation sensitized by the UV/H_2O_2 process.

In the UV/H_2O_2 treatments of acetone carried out on industrial waters, it has been found that acetone treats more slowly than other similar pollutants, such as 1,4-dioxane or

S0013-936X(95)00866-2 CCC: $12.00

methyl ethyl ketone. The present work was undertaken to study the kinetics and mechanism of acetone degradation in dilute aqueous solution, sensitized by hydrogen peroxide photolysis, with the aim of explaining why its treatment is slow. In this respect, the acetone decay was followed concomitantly with the growth and decay of reaction intermediates until complete mineralization was achieved. The roles of some parameters, such as the pH and the initial concentrations of acetone and H_2O_2, were examined in order to provide a full description of this system. A mechanism has been proposed that accounts for the observed behavior of the system.

Experimental Section

Reagents and Materials. Acetone (99.5%, BDH, suitable for spectrophotometry and chromatography) and hydrogen peroxide (30%, Caledon, analytical reagent grade) were used as received. The 0.1000 N ceric sulfate solution in 0.1 N H_2SO_4 was provided by VWR Scientific. Catalase from bovine liver, 19 900 unit mg^{-1} (1 unit decomposes 1 μmol H_2O_2/min at pH 7.0, at 25 °C) was obtained from Sigma. Deionized water has been used in all experiments and analytical determinations.

Apparatus. The UV irradiations were carried out in a stainless steel Rayox reactor provided by Solarchem Environmental Systems of Markham, Ontario, Canada. This unit consists of a batch tank of 28 L capacity, a recycle pump, and a Rayox UV reactor (6.5 L). The pump draws the pollutant solution from the batch tank and pumps it through the reactor and back to the batch tank at a controlled flow rate. The recycle loop contains a flow meter (0−180 L min^{-1}), a heat exchanger/static mixer, a sample port, and a pH meter.

The Rayox reactor contains a Solarchem 1 kW medium pressure mercury lamp with a known spectral distribution and output. The lamp is separated from the water by a quartz sleeve of 4.2 cm diameter. The mean effective path length between the quartz sleeve and the reactor wall is 7.0 cm, allowing for a reasonable fraction of light to be absorbed. The total photon flux entering the reactor from the UV lamp was found to be $G_o = (6.45 \pm 0.16) \times 10^{-4}$ Einstein s^{-1} in the wavelength range of 200−500 nm and $(2.93 \pm 0.08) \times 10^{-4}$ Einstein s^{-1} from 200 to 300 nm (*21*) as determined with a 0.15 M potassium ferrioxalate actinometer (*22*) and the known spectral distribution of the lamp emission.

In all experiments, we used a total reaction volume of 28 L, circulated at a flow rate of 110 L min^{-1}. Experiments conducted at flow rates of 40, 75, and 110 L min^{-1} established that the observed kinetics are independent of flow rate. This high flow rate also assures turbulent flow through the reactor. Samples were taken at various exposure times and then analyzed.

In order to check if acetone is stripped out from the bulk of the solution as a pumping effect, a few "dark" control experiments at the above flow rate, covering the range of acetone concentration 0.35−3.5 mM were carried out. No significant depletion in acetone concentration, as measured by GC, was observed over a 60 min period.

Fraction of UV Absorbed. For modeling purposes, it is important to calculate the fraction of UV (200−300 nm) absorbed when two absorbers are present. To do this, the known spectral distribution of the lamp (as modified by transmittance of the quartz sleeve) was divided into 5 nm bands, within which the light was assumed to be monochromatic. Using Beer's law, the photon flux absorbed in the effective path length of 7.0 cm (determined using a linear multiple point source model for the lamp) was calculated in each band. This absorbed photon flux was assigned to each absorber in proportion to its absorbance. The fraction of light absorbed by each absorber is then its integrated absorbed photon flux divided by the integrated incident lamp flux.

Analytical Determinations. Hydrogen peroxide was analyzed by titration with ceric sulfate solution (*23*). Acetone concentrations were determined by a gas chromatographic method, using a Perkin Elmer (Sigma 2B) gas chromatograph, equipped with a flame ionization detector. A high-performance gas chromatograph DB 624 glass capillary column (30 m × 0.53 mm) and a guard column (J&W Scientific) were utilized. The injector and detector temperatures were 220 °C, and the column temperature was set at 40 °C. The pressure of the carrier gas (helium) at the instrument was 90 kPa. For these experimental conditions, the retention time of acetone was 1.3 min. A Hewlett Packard HP 3396 Series II integrator was employed to provide retention time and peak area data from the GC detector.

Acetic, formic, and oxalic acids were analyzed using ion-exchange separation combined with suppressed conductivity detection performed with a Dionex DX-100 ion chromatograph provided with the AI-450 software program. The conditions used were as follows: Ion Pac AS10 (4 × 250 mm) analytical column protected by an Ion Pac AG4A (4 × 50 mm) guard column, eluent solution of 90 mM sodium hydroxide in deionized water at an isocratic flow rate of 1 mL min^{-1}, regenerant solution of 25 mM sulfuric acid at a flow rate of 6.5 mL min^{-1}. The operating pressure of the system was set at 2040 psi, the background conductivity at 9 μS, and the full conductivity scale at 30 μS. The sample loop was 50 μL, and the injected volume was 1 mL.

By using such a strong basic eluent, hydrogen peroxide was ionized to HO_2^- [$pK_a = 11.8$ (*24*)] and eluted from the column as a broad peak interfering with the acetate and formate ion peaks. This imposed the requirement that the hydrogen peroxide be destroyed by addition of 4 μL of catalase solution into a 5 mL sample before analysis. According to the above settings, the following retention times were obtained: 2.57 min (acetate), 3.05 min (formate), and 20.57 min (oxalate).

Total organic carbon (TOC) was determined with a Shimadzu TOC-5050 total organic carbon analyzer with an integrated ASI-5000-S autosampler. This analyzer measured the levels of CO_2 gas produced during the catalytic combustion of organic carbon-containing compounds in the water samples.

Results and Discussion

Both hydrogen peroxide and acetone are weakly absorbing compounds in the UV range. For example, at $\lambda = 254$ nm, the molar absorption coefficients are $\epsilon = 18.4$ M^{-1} cm^{-1} (*25*) and $\epsilon = 16.0$ M^{-1} cm^{-1} for hydrogen peroxide and acetone, respectively (Figure 1). In the case of H_2O_2, the absorption increases as the wavelength decreases. However, in dilute aqueous solutions of acetone (~1 mM) in the presence of various concentrations of hydrogen peroxide (3−16 mM), H_2O_2 is the principal absorber of UV light, so that the direct photolysis of acetone can be neglected.

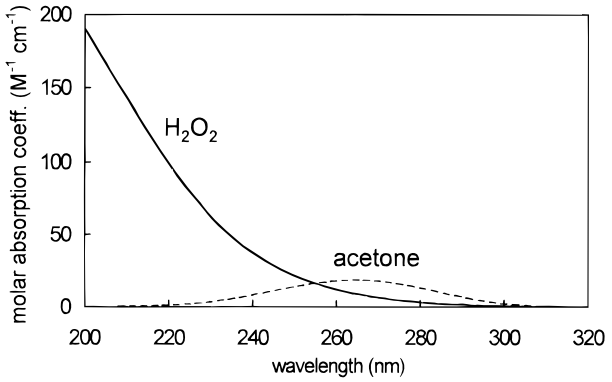

FIGURE 1. Spectral distribution of molar absorption coefficients of hydrogen peroxide (*25*) and acetone in distilled water.

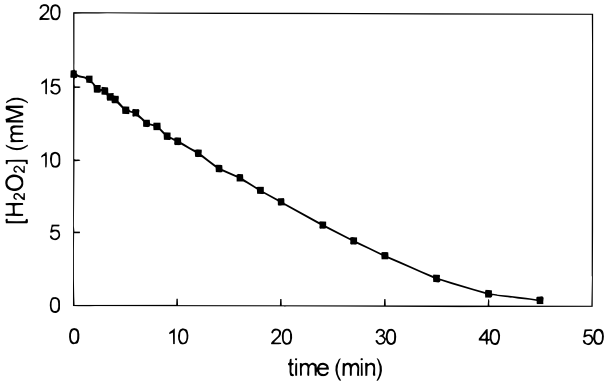

FIGURE 2. Direct photolysis of hydrogen peroxide; $[H_2O_2]_o = 15.87$ mM, $G_o = 2.93 \times 10^{-4}$ Einstein s^{-1}.

Direct Photolysis of Hydrogen Peroxide. The photolysis of hydrogen peroxide in pure water has been studied extensively by various groups of researchers in the 1950s (*25*−*28*) in order to elucidate the reaction mechanism and to determine the primary and overall quantum yields. The general consensus is that the reaction scheme below describes H_2O_2 photodecomposition in pure water:

$$H_2O_2 + h\nu \rightarrow 2{\cdot}OH \qquad \phi_{OH}FG_o/V \qquad (1)$$

$$\cdot OH + H_2O_2 \rightarrow HO_2\cdot + H_2O \qquad (2)$$

$$k_{H_2O_2} = 2.7 \times 10^7\ M^{-1}\ s^{-1}\ (29)$$

$$HO_2\cdot + \cdot OH \rightarrow H_2O + O_2 \qquad (3)$$

$$k = 6 \times 10^9\ M^{-1}\ s^{-1}\ (29)$$

$$HO_2\cdot + HO_2\cdot \rightarrow H_2O_2 + O_2 \qquad (4)$$

$$k = 8.3 \times 10^5\ M^{-1}\ s^{-1}\ (30)$$

where ϕ_{OH} is the primary quantum yield of ·OH radical generation, F is the fraction of UV light absorbed by H_2O_2, G_o is the total incident UV photon flux, and V is the total irradiated volume. The net reaction from this scheme is

$$2H_2O_2 + h\nu \rightarrow 2H_2O + O_2 \qquad (5)$$

so that the overall quantum yield for H_2O_2 destruction (∼1.0) is twice the primary quantum yield (0.5) for H_2O_2 removal by reaction 1, as reported in the literature (*25*−*28*).

Thus, H_2O_2 photolysis generates the very highly oxidizing and reactive ·OH radicals, which are involved in the fast degradation of organic pollutants (e.g., acetone). Figure 2 shows the experimental data obtained during the irradiation

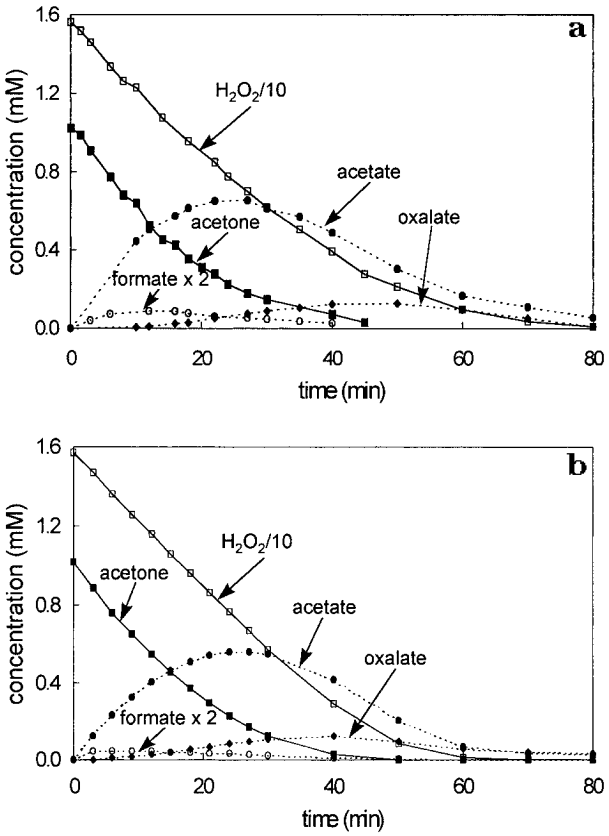

FIGURE 3. Acetone and H_2O_2 decay and the time course of reaction intermediates evolved during UV/H_2O_2 treatment: (a) experimental data; (b) computed data from the kinetic model. Each minute corresponds to 0.595 kWh of electrical energy used per m^3 of water treated.

of a 15.9 mM hydrogen peroxide aqueous solution. The photolysis follows zero-order kinetics over the first 20 min, with a rate of $(7.2 \pm 0.35) \times 10^{-6}$ M s^{-1}.

Degradation of Acetone Sensitized by Hydrogen Peroxide under UV Light. *Acetone Degradation and Reaction Intermediates.* Figure 3, panel a (experimental data) and panel b (computer-modeled data), show the photochemical behavior of a mixture of 1.02 mM acetone and 15.6 mM H_2O_2 in aqueous solution. At these relative concentrations, most of the incident UV flux is absorbed by H_2O_2 (83.1%) as compared with acetone (4.7%), so that both acetone and reaction intermediates are destroyed primarily by means of the ·OH radicals generated from the photolysis of H_2O_2 and not by direct photolysis.

The acetone decay follows first-order kinetics with an observed rate constant of $k = (1.13 \pm 0.06) \times 10^{-3}$ s^{-1}, while that of hydrogen peroxide obeys zero-order kinetics over the first 30 min with a rate of $(5.8 \pm 0.5) \times 10^{-6}$ M s^{-1}, which is ∼20% lower than that found with H_2O_2 alone in water. This suggests a competition for ·OH radicals between H_2O_2 and other scavengers, such as acetone and its byproducts.

During the experiment, the pH dropped rapidly from 6.0 ($t = 0$ min) to 3.6 ($t = 30$ min) and then increased slowly to 5.0 ($t = 90$ min). This variation is explained by the formation of some carboxylic acids, identified as formic, acetic, and oxalic acids, and by the complete mineralization of these compounds to carbon dioxide and water by the end of the irradiation period.

From Figure 3a, one can conclude that the primary intermediates are formic and acetic acids, while oxalic acid is generated later, probably from the decomposition of

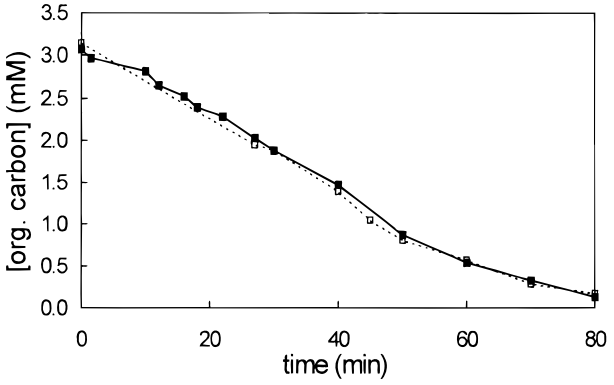

FIGURE 4. Total organic carbon balance during the acetone degradation by UV/H_2O_2 treatment: (■) TOC calculated as TOC, mM = 3 [acetone, mM] + 2 [acetic acid, mM] + 2 [oxalic acid, mM] + [formic acid, mM]; (□) TOC measured experimentally.

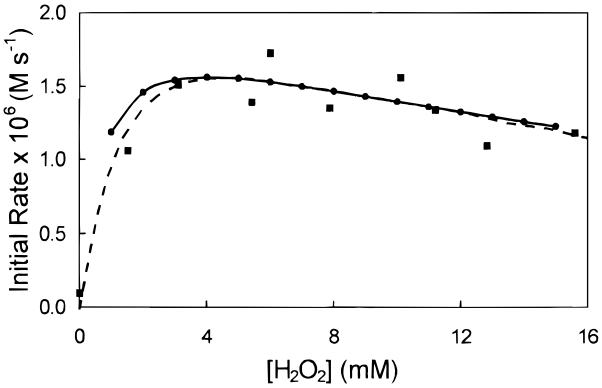

FIGURE 5. Initial rate of acetone degradation as a function of the initial hydrogen peroxide concentration: (■) experimental data; (●) computed data; $[acetone]_o \approx 1$ mM.

acetic acid, since the highest concentration of oxalic acid is reached at irradiation times when acetone is completely destroyed.

On the other hand, the dynamics of the system consisting of reagents (acetone and H_2O_2) and byproducts (carboxylic acids) toward the complete destruction of each component is governed by their relative concentrations, the pH, the pK_a of each byproduct (*31*), and the rate constants of various components with ·OH radicals (*29*).

It seems that, even at relatively short irradiation times, the intermediates formed in low concentrations can compete efficiently with acetone for ·OH radicals, which could explain the slowness of acetone treatment driven by UV/H_2O_2 in dilute aqueous solution.

Based on an assumed mechanism (see below) and a set of reaction rate constants and known pK_a values, we have carried out a kinetic simulation (described below) of this system. The results are shown in Figure 3b. Given the uncertainties in the literature values of the reaction rate constants, we consider the fit to be reasonable.

The total organic carbon concentration, determined experimentally by carbon analysis, agrees very well with that calculated using the concentrations of acetone, formic acid, acetic acid, and oxalic acid, considered as the only organic compounds present in the system (Figure 4). This suggests that no other major organic intermediates are formed in significant concentrations. Moreover, the low TOC value at the longest irradiation time confirms the assumption already predicted by the pH, namely, that all the organics are almost completely oxidized to CO_2 and H_2O. An electrical energy per mass of 1268 kWh/kg was calculated from the observed zero-order decay of the TOC and corresponds to the electrical energy required to bring about the degradation of 1 kg of carbon in organic compounds expressed as TOC, in the studied system.

Effect of pH. As mentioned above, during the irradiation period of the acetone/hydrogen peroxide system, the pH changes because of organic acid formation. In order to check the role of pH on the initial rate of acetone decay, some experiments were performed on ~1 mM acetone and ~16 mM H_2O_2 in aqueous solution at certain controlled pH values, adjusted with 1 M H_2SO_4 or 1 M NaOH solutions.

The initial rate of acetone removal [$(1.2 \pm 0.09) \times 10^{-6}$ M s^{-1}] was found to be independent of pH in the range 2−7. At pH 10, a lower initial rate [$(2.9 \pm 0.23) \times 10^{-7}$ M s^{-1}] was found. This could be explained in terms of hydrogen peroxide dissociation (reaction 6) in alkaline media. The rate constant of reaction 7 between ·OH radicals and hydroperoxide ion is much higher than that of ·OH with hydrogen peroxide (*29*). This reduces the effectiveness of ·OH radical attack on acetone molecules:

TABLE 1

Fraction of UV Light Absorbed and Quantum Yield of Acetone Degradation (~1 mM) in the Presence of Various Concentrations of H_2O_2

H_2O_2, mM	fraction of UV absorbed (%)	$\phi_{acetone}$
0	13.4	0.053[a)]
1.52	57.1	0.150
2.97	67.8	0.180
5.42	76.5	0.156
7.87	81.2	0.143
10.06	83.8	0.161
11.12	84.8	0.144
12.82	86.1	0.112
15.71	87.8	0.117

[a] The literature value is 0.061 (*19*).

$$H_2O_2 \rightleftharpoons H^+ + HO_2^- \qquad pK_a = 11.8\ (24) \qquad (6)$$

$$\cdot OH + HO_2^- \rightarrow \cdot O_2^- + H_2O \qquad (7)$$

$$k = 7.5 \times 10^9\ M^{-1}\ s^{-1}\ (pH\ 7.7{-}11)\ (29)$$

No significant change of the initial rate of H_2O_2 decay in the presence of acetone was observed in the pH range 2−7 [$(6.2 \pm 0.3) \times 10^{-6}$ M s^{-1}], but a higher value [$(7.6 \pm 0.42) \times 10^{-6}$ M s^{-1}] was found at pH 10, supporting the above explanation. In conclusion, no acid-catalyzed reaction occurs in the photochemical oxidation mechanism of acetone in the presence of hydrogen peroxide in the pH range 2−7.

Effect of the Initial Concentration of Hydrogen Peroxide. The initial rate of acetone degradation sensitized by the UV photolysis of H_2O_2 depends on the hydrogen peroxide concentration, as shown in Figure 5. The fraction of UV light absorbed and the calculated quantum yields of acetone degradation corresponding to the data plotted in Figure 5 are given in Table 1.

The experimental data shown in Figure 5 are in good agreement with those calculated from the computer model. The optimum range of H_2O_2 concentrations seems to be 4−7 mM. At lower concentrations, H_2O_2 absorbs only a small fraction of the incident light, and so the initial rate of acetone removal is slow. At higher concentrations, H_2O_2

becomes a strong scavenger for ·OH radicals, competing with acetone, and hence the initial rate of acetone degradation decreases. Glaze *et al.* (*10*) observed a similar effect in the treatment of 1,2-dibromo-3-chloropropane. From Table 1, one observes the significant difference in acetone quantum yields with and without H_2O_2.

In order to ensure a complete mineralization of all intermediates formed in the system, a certain H_2O_2 concentration is necessary. This was the reason for using about 16 mM H_2O_2 in our experiments.

Effect of the Initial Acetone Concentration. For a given hydrogen peroxide concentration (~15.5 mM), the initial rates of both acetone and hydrogen peroxide degradation depend on the initial concentration of acetone (Table 2).

As the acetone concentration increases, the initial rate of hydrogen peroxide decay decreases because acetone molecules compete more efficiently with H_2O_2 molecules for ·OH radicals. In the range of relative concentrations of acetone and hydrogen peroxide, where $k_{ac}[CH_3COCH_3]$ is much higher than $k_{H_2O_2}[H_2O_2]$ (see eq 9), zero-order kinetics for acetone decay should be observed, and then the initial rate of H_2O_2 decay should be half that of acetone because reaction 2 is mostly inhibited. That is what we observed in the system 4.5 mM acetone/3.0 mM H_2O_2 under UV light, where the initial rate of acetone decay was found to be $(2.7 \pm 0.06) \times 10^{-6}$ M s^{-1}, while that of hydrogen peroxide was $(1.2 \pm 0.1) \times 10^{-6}$ M s^{-1}.

Also, as shown in Table 2, the rate constant for acetone degradation decreases as the acetone concentration increases, suggesting that the generated intermediates, especially formic acid, become increasingly important scavengers of ·OH radicals.

At short irradiation times, where acetone and hydrogen peroxide can be considered the only effective ·OH radical scavengers, a steady-state kinetic analysis can be considered on the basis of the following simple reaction scheme:

$$H_2O_2 + h\nu \rightarrow 2{\cdot}OH \qquad \text{rate} = \phi_{OH} F G_o / V \qquad (1)$$

$$\cdot OH + CH_3COCH_3 \xrightarrow{k_{ac}} \cdot CH_2COCH_3 + H_2O \qquad (8)$$

$$k_{ac} = 1.1 \times 10^8 \text{ M}^{-1} \text{ s}^{-1} \ (29)$$

$$\cdot OH + H_2O_2 \xrightarrow{k_{H_2O_2}} H_2O + HO_2\cdot \qquad (2)$$

where k_{ac} and $k_{H_2O_2}$ are the rate constants for reactions 8 and 2, respectively.

In the steady-state approximation, $d[\cdot OH]/dt = 0$, and the final kinetic expression extrapolated to time $t = 0$ can be written as

$$-\left.\frac{d[CH_3COCH_3]}{dt}\right|_{t=0} = \frac{k_{ac}[CH_3COCH_3]_o \phi_{OH} F G_o / V}{k_{ac}[CH_3COCH_3]_o + k_{H_2O_2}[H_2O_2]_o} \qquad (9)$$

where $\{-d[CH_3COCH_3]/dt\}|_{t=0}$ denotes the initial rate of acetone degradation.

Within the acetone concentration range used, there is a linear dependence of the initial rate of acetone degradationon the function

$$M = \frac{k_{ac}[CH_3COCH_3]_o}{k_{ac}[CH_3COCH_3]_o + k_{H_2O_2}[H_2O_2]_o} \qquad (10)$$

as shown in Figure 6 (correlation coefficient 0.976). This behavior confirms the validity of the steady-state approximation at short exposure times.

TABLE 2

Initial Rate of Acetone and Hydrogen Peroxide Decays at Various Concentrations of Acetone

[acetone] (mM)	[H_2O_2] (mM)	F (%)[a]	initial rates $\times 10^6$ (M s^{-1}) acetone	H_2O_2	k $\times 10^3$ (s^{-1})[b]
0.000	15.71	86.2	0	7.76	
0.369	15.21	84.7	0.52		1.42
0.448	15.50	84.7	0.61		1.36
0.682	15.55	84.0	0.75	6.3	1.10
1.024	15.61	83.1	0.95	5.8	1.13
1.114	15.71	82.9	1.05		0.94
1.652	15.38	81.2	1.52	5.7	0.92
2.340	15.31	79.4	1.66		0.71
2.436	15.30	79.1	1.75	5.3	0.72
3.362	15.70	77.3	2.37		0.65
3.628	15.30	76.4	2.12	4.3	0.58

[a] Fraction of UV light absorbed by hydrogen peroxide. [b] Rate constant for the first-order kinetics of the acetone degradation process.

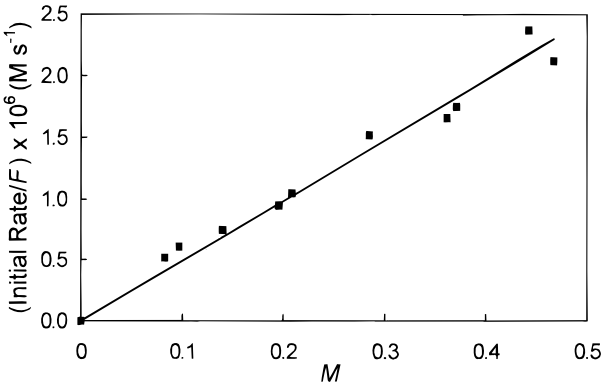

FIGURE 6. Effect of the initial concentration of acetone on the initial rate of acetone decay in the steady-state approximation (see eq 9).

From the slope of the plot of the initial rate versus M (Figure 6), the product $\phi_{OH}G_o = 1.63 \times 10^{-4}$ Einstein s^{-1} can be calculated, which is significantly lower than that expected (2.93×10^{-4} Einstein s^{-1}), derived from the well-established $\phi_{OH} = 1.0$ and the actinometrically measured value of G_o. This discrepancy probably arises from some factors related to the experimental conditions we used, such as polychromatic light, recirculating batch reactor, some possible inhomogeneity of light absorption inside the reactor, and acetone may be recycled to a some extent in the studied system (see reaction 25). If we assume that the product $\phi_{OH}G_o$ is ~20% less than that expected and that about one-third of the acetone is recycled, we can obtain agreement with the slope of Figure 6.

To justify the above points, we note that experiments carried out on photolysis of ~16 mM H_2O_2 in aqueous solution, under identical conditions, led to a consistent calculated $\phi_{OH}G_o$ value of 2.34×10^{-4} Einstein s^{-1}, which corresponds to only 80% of the expected value. On the other hand, acetone recycling is an important step in the reaction mechanism, as suggested by the kinetic simulations. In such a complicated system involving many reaction steps and possible experimental errors, we consider the difference between ~33% and 43% acetone recycling, as proposed above and by the kinetic model respectively, to be an acceptable one. More investigations concerning these explanations will be carried out in future experiments.

Mechanism of Acetone Degradation Sensitized by the Photolysis of H_2O_2. The experimental results provide information of importance to understanding the mechanism of acetone degradation under the UV/H_2O_2 treatment. The following proposed reaction scheme is consistent with our observations.

The initial photochemical step in the acetone/H_2O_2 system consists of hydrogen peroxide photolysis generating ·OH radicals (reaction 1), which then by hydrogen abstraction from acetone molecules initiate the decomposition by reaction 8:

$$H_2O_2 + h\nu \rightarrow 2{\cdot}OH \quad (1)$$

$$\cdot OH + CH_3COCH_3 \rightarrow \cdot CH_2COCH_3 + H_2O \quad (8)$$

The acetonyl radical reacts with oxygen by a diffusion-controlled process forming peroxy radicals (reaction 11), which can react by one of two routes. A radical−radical reaction (reaction 12) followed by a β-scission in reaction 13 and oxidation of formaldehyde to formic acid in reaction set 14−16 should give some of the observed intermediates:

$$\cdot CH_2COCH_3 + O_2 \rightarrow \cdot OOCH_2COCH_3 \quad (11)$$

$$k = 3 \times 10^9\ M^{-1}\ s^{-1}\ (32)$$

$$2{\cdot}OOCH_2COCH_3 \rightarrow 2{\cdot}OCH_2COCH_3 + O_2 \quad (12)$$

$$2k = 8 \times 10^8\ M^{-1}\ s^{-1}\ (32)$$

$$\cdot OCH_2COCH_3 \xrightarrow[\beta\text{-scission}]{} HCHO + \cdot COCH_3 \quad (13)$$

$$HCHO + H_2O \rightarrow CH_2(OH)_2 \quad (14)$$

$$HOCH_2OH + \cdot OH \rightarrow \cdot OCH_2OH(HO\dot{C}HOH) + H_2O \quad (15)$$

$$\cdot OCH_2OH(HO\dot{C}HOH) + O_2 \rightarrow HO_2{\cdot} + HCOOH \quad (16)$$

or, alternatively, a six-membered atom rearrangement (reaction 17) followed by a β-scission can lead to ketene, which then hydrolyses to acetic acid (reaction 18), a well-known reaction in aqueous solution (*18*):

$$\cdot OOCH_2COCH_3 \rightarrow [HOOCH_2COCH_2{\cdot}] \rightarrow \cdot CH_2OOH + CH_2CO \quad (17)$$

$$CH_2CO + H_2O \rightarrow CH_3COOH \quad (18)$$

$$\cdot CH_2OOH + O_2 \rightarrow HCOOH + HO_2{\cdot} \quad (19)$$

Acetyl radicals formed in reaction 13 can dissociate (reaction 20) or react with oxygen (reaction 22):

$$\cdot COCH_3 \rightarrow CO + CH_3{\cdot} \quad (20)$$

$$CH_3{\cdot} + O_2 \rightarrow CH_3OO{\cdot} \quad (21)$$

$$\cdot COCH_3 + O_2 \rightarrow \cdot OOCOCH_3 \quad (22)$$

$$CH_3OO{\cdot} + \cdot OOCOCH_3 \rightarrow HCHO + CH_3COOH + O_2 \quad (23)$$

generating formaldehyde and acetic acid in a 1:1 ratio.

Formaldehyde generated by reactions 13 and 23 follows essentially the reaction set 14−16 but also can be oxidized to formic acid directly by the dissolved oxygen under UV light. A test experiment done on dilute formaldehyde aqueous solution proved the occurrence of reaction 24:

$$2HCHO + O_2 \xrightarrow{h\nu} 2HCOOH \quad (24)$$

Another possible route followed by acetonyl radicals is reaction with $HO_2{\cdot}$ radicals generated during the photolysis of H_2O_2. The concentration of $HO_2{\cdot}$ radicals can reach values of 10^{-6}−10^{-5} M, and considering the high rates of radical-radical reactions, these radicals can compete with O_2, thus regenerating acetone:

$$\cdot CH_2COCH_3 + HO_2{\cdot} \rightarrow CH_3COCH_3 + O_2 \quad (25)$$

Reaction 25 is also predicted by the computer simulations.

Dilute aqueous solutions of acetone have been studied by γ-radiolysis and pulse radiolysis under conditions where hydroxyl radicals are the major reactive species (*32*). Here, the principal reaction products observed were methylglyoxal, hydroxyacetone, formaldehyde, and hydrogen peroxide. Although under our experimental conditions hydroxyl radicals are also the major reactive species, the conditions are different since we have a large concentration of H_2O_2 and strong UV irradiation. Thus, one should not expect that the same products would be formed.

Even at low concentrations, formic acid (formate) competes efficiently for ·OH radicals, as compared to H_2O_2 or acetone, because of the high rate constant of the following process:

$$\cdot OH + HCOOH\ (HCOO^-) \rightarrow H_2O + \cdot COOH\ (\cdot COO^-) \quad (26)$$

There are two possible reaction paths for the oxidation of the ·COOH radicals to CO_2:

$$\cdot COOH(\cdot COO^-) + O_2 \rightarrow CO_2 + HO_2{\cdot}(O_2{\cdot}^-)\ (33) \quad (27)$$

$$\cdot COOH + H_2O_2 \rightarrow CO_2 + H_2O + \cdot OH\ (34) \quad (28)$$

Reaction 28 is very similar to the reaction between $HO_2{\cdot}$ and H_2O_2 (see reaction 41 in Table 3), where $k = 3.7\ M^{-1}\ s^{-1}$ (*35*). Even though the ratio $[H_2O_2]/[O_2]$ during the irradiation time is in the range 10−100, we propose that the rate constant for reaction 28 is small, and thus almost all ·COOH radicals convert to CO_2 via reaction 27.

Since acetic acid is less reactive with ·OH radicals than formic acid, it increases in concentration as long as the acetone concentration is still high and formic acid is present in solution. When the concentration of CH_3COOH is much greater than that of CH_3COCH_3, acetic acid becomes a good scavenger of ·OH radicals competing with acetone and hydrogen peroxide. Its degradation probably goes through glycolic acid and glyoxylic acid (reaction 31) as intermediates in the formation of oxalic acid:

$$\cdot OH + CH_3COOH \rightarrow \cdot CH_2COOH + H_2O \quad (29)$$

$$\cdot CH_2COOH + O_2 \rightarrow \cdot OOCH_2COOH \quad (30)$$

$$2{\cdot}OOCH_2COOH \xrightarrow{\text{disproportionation}} HOOCCHO + HOCH_2COOH + O_2 \quad (31)$$

Reaction 31 was also proposed by Schuchmann *et al.* (*36*). They also proposed another possible reaction path

TABLE 3

Reactions Used in the Kinetic Model

no.	reaction[a]	rate constant (M^{-1} s^{-1})	pK_a
(1)	$H_2O_2 + h\nu \rightarrow 2{\cdot}OH$		
(2)	$\cdot OH + H_2O_2 \rightarrow HO_2\cdot + H_2O$	2.7×10^7 (*29*)	
(40)	$\cdot OH + \cdot OH \rightarrow H_2O_2$	1.1×10^{10} (*29*)	
(4)	$HO_2\cdot + HO_2\cdot \rightarrow H_2O_2 + O_2$	8.3×10^5 (*30*)	4.8 (*30*)
(41)	$HO_2\cdot + H_2O_2 \rightarrow H_2O + O_2 + \cdot OH$	3.7 (*35*)	
(3)	$HO_2\cdot + \cdot OH \rightarrow H_2O + O_2$	6×10^9 (*29*)	
(8)	$\cdot OH + CH_3COCH_3 \rightarrow \cdot CH_2COCH_3 + H_2O$	1.1×10^8 (*29*)	
(11)	$\cdot CH_2COCH_3 + O_2 \rightarrow \cdot OOCH_2COCH_3$	3×10^9 (*32*)	
(25)	$\cdot CH_2COCH_3 + HO_2\cdot \rightarrow CH_3COCH_3 + O_2$	(3×10^{11})[b]	
(26)	$\cdot OH + HCOOH \rightarrow \rightarrow CO_2 + H_2O + HO_2\cdot$	1.3×10^8 (*29*)	3.75 (*31*)
(42)	$\cdot OH + HCOO^- \rightarrow \rightarrow CO_2 + H_2O + O_2\cdot^-$	3.2×10^9 (*29*)	
(29)	$\cdot OH + CH_3COOH \rightarrow \rightarrow HOOCCOOH$ $\rightarrow \rightarrow HCOOH$	1.6×10^7 (*29*)	4.75 (*31*)
(43)	$\cdot OH + CH_3COO^- \rightarrow \rightarrow HOOCCOO^-$ $\rightarrow \rightarrow HCOO^-$	8.5×10^7 (*29*)	
(36)	$HOOCCOOH + \cdot OH \rightarrow \rightarrow 2CO_2 + H_2O + HO_2\cdot$	1.4×10^6 (*29*)	1.23 (*31*)
(44)	$HOOCCOO^- + \cdot OH \rightarrow \rightarrow 2CO_2 + H_2O + O_2\cdot^-$	4.7×10^7 (*29*)	4.19 (*31*)
(45)	$H^+ + {}^-OOCCOO^- + \cdot OH \rightarrow \rightarrow 2CO_2 + H_2O + O_2\cdot^-$	7.7×10^6 (*29*)	

[a] The reaction numbers correspond to those in the text. However, here they refer to overall reactions which may contain several primitive steps.
[b] See text, Kinetic Simulations section.

starting from acetate peroxyl radicals and leading to formaldehyde:

$$2{\cdot}OOCH_2COOH \rightarrow \rightarrow 2{\cdot}OCH_2COOH + O_2 \quad (32)$$

$$\cdot OCH_2COOH \rightarrow HCHO + \cdot COOH \quad (33)$$

Under our conditions, formaldehyde would be oxidized to formic acid (reaction set 14−16) and carboxyl radicals to CO_2 (reaction 27).

In such an oxidizing medium, both glyoxylic acid and glycolic acid should be mainly oxidized by reaction with ·OH radicals, followed by subsequent reaction with oxygen or partially converted to oxalic acid, perhaps by the photochemical step:

$$\left.\begin{matrix} HOOCCHO \\ HOOCCH_2OH \end{matrix}\right\} \xrightarrow{[O_2],\ h\nu} HOOCCOOH \quad (34)$$

Ogata *et al.* (*34*) detected glycolic, formic, and tartaric (trace) acids, along with methane (trace) and CO_2, during the irradiation of aqueous solutions of acetic acid in the presence of four times excess of hydrogen peroxide. They used a Halos 60 W low-pressure Hg lamp at 20 °C. No oxalic acid formation was mentioned in their work.

Under our experimental conditions, where after 27 min of irradiation the maximum concentration of CH_3COOH (∼0.65 mM) was reached and the H_2O_2 concentration was almost 10 times higher, no direct photolysis of acetic acid can be expected (which is responsible for CH_4 and CO_2 formation directly from acetic acid).

Reaction 35, proposed by Ogata *et al.* (*34*), cannot be excluded, and the small amount of formic acid that we detected at longer irradiation times (30−40 min) may arise from glyoxylic acid decomposition:

$$OHCCOOH + H_2O_2 \xrightarrow{\text{dark}} HCOOH + CO_2 + H_2O \quad (35)$$

Moreover, by a test experiment done on an acetic acid solution in the presence of H_2O_2 under UV light, we observed the generation of formic acid and oxalic acid. The concentration of formic acid was very low because of its high reactivity toward ·OH radicals. However, according to the growth of oxalic acid concentration in acetone/H_2O_2/UV system, we presume that reaction set 34 competes efficiently with reaction 35.

Oxalic acid decomposition is mediated by reaction with ·OH radicals leading to CO_2 and H_2O (see also reaction 27):

$$HOOCCOOH + \cdot OH \rightarrow CO_2 + H_2O + \cdot COOH \quad (36)$$

At long irradiation times, the only products reacting with ·OH radicals are oxalic acid and acetic acid. The corresponding rate constants are of the same order of magnitude so that, at the relative concentrations found in our system, oxalic acid and acetic acid decay at similar rates.

Kinetic Simulations. In order to provide a more sophisticated model than that resulting from an analytical application of the steady-state model, we have employed a numerical simulation using a simple finite-difference method to solve the coupled differential equations arising from the kinetic scheme. We employed the steady-state approximation for the acetonyl and hydroxyl radicals (butnot for $HO_2\cdot$) in a manner similar to that used by Glaze *et al.* (*10*). The steady-state concentrations are

$$[\cdot OH] = (F\phi_{OH}G_o + k_{41}[H_2O_2][HO_2\cdot])/\Sigma \quad (37)$$

where

$$\Sigma = k_2[H_2O_2] + k_3[HO_2\cdot] + k_8[CH_3COCH_3] + k_{29}[CH_3COOH] + k_{43}[CH_3COO^-] + k_{26}[HCOOH] + k_{42}[HCOO^-] + k_{36}[HOOCCOOH] + k_{44}[HOOCCOO^-] + k_{45}[{}^-OOCCOO^-] + k_{40}[\cdot OH] \quad (38)$$

and

$$[\cdot CH_2COCH_3] = k_8[CH_3COCH_3]/(k_{11}[O_2] + k_{25}[HO_2\cdot]) \quad (39)$$

The pH of the reaction mixture, which varies along with the concentration of carboxylic acids, and the percent dissociation for each ionizable species were calculated at every time step. The light absorbed by hydrogen peroxide in the presence of the other stable species was calculated from the wavelength-dependent absorption coefficients and

lamp intensity profile also at each time step. After trials involving smaller time increments were found to give identical results, the time interval was chosen to be 0.25 s. All of the data used for the simulations are collected in Table 3.

Kinetic simulations, in general, are independent of many of the details of the proposed reaction scheme. Thus, for instance, the exact sequence of reactions leading from acetic acid to oxalic acid is irrelevant as long as no stable intermediates are formed and no intermediates couple this reaction to others outside the acetic acid/oxalic acid "black box". On the other hand, the photolysis of hydrogen peroxide is an example where the details are relevant, since the hydroxyl radicals couple this reaction to many others.

Simulations of the photolysis of hydrogen peroxide in the absence of acetone involved the reactions 1−4 as well as reactions 40 and 41 in Table 3. Reaction 41 is a chain propagation step that results in a quantum yield for hydrogen peroxide destruction greater than one under low light flux conditions. By contrast, reaction 40 results in a quantum yield less than one for very high light intensities. Under our conditions, these latter two reactions had a negligible effect. As discussed previously, this entire set of reactions gives a quantum yield of unity for hydrogen peroxide destruction. However, our experimental results could only be fit if the quantity $\phi_{OH}G_o$ was reduced to 80% of its expected value. Either the primary quantum yield for hydroxyl radical production had to be reduced to 0.80 or, if the literature value of 1.0 is accepted, the value for G_o is only 80% of that measured by actinometry. The value for $\phi_{OH}G_o$ measured in our experiments on hydrogen peroxide photolysis was used in our acetone simulations.

The initial simulations did not include the acetone recycling reaction 25, and the calculated rate of disappearance of acetone was much greater than that observed. Attempts to modify our reaction scheme by including steps such as

$$2\cdot OH + CH_3COCH_3 \rightarrow \text{products} \qquad (46)$$

reduced the discrepancy only slightly and also led to decreased hydrogen peroxide destruction. Once recycling was introduced, reasonable agreement for both acetone and hydrogen peroxide destruction rates could be obtained.

If acetic acid destruction is considered to go entirely by way of oxalic acid, the concentration of oxalic acid was calculated to be approximately twice that observed. Introducing a branching reaction, such that half of the acetic acid forms oxalic acid while the other half generates formic acid, solved this problem. This branching is supported by experimental results that detected formic acid and oxalic acid when aqueous acetic acid was photolyzed in the presence of hydrogen peroxide.

The overall agreement of the simulation results with the observed data leads us to believe that the scheme is essentially correct. However, the fraction of acetone that we require to be recycled (43% at the beginning of the reaction) is surprisingly large.

The value of the rate constant for acetone recycling as reported in Table 3 is unrealistically large and is a result of a computational artifact. Our simulation uses the average light flux, whereas the actual experimental equipment has a separate reactor and reservoir. Moreover, the illumination of the reactor from a central UV lamp is nonuniform. Since the rate of radical−radical reactions depends essentially on the square of the light intensity, both of these details lead to higher real rates of radical−radical reactions than in our simulation. In order to agree with experiment, the simulation must compensate by using a much larger assumed value for the associated rate constant (reaction 25).

Acknowledgments

This work was supported financially by a Collaborative Research and Development Grant jointly funded by the Natural Sciences and Engineering Research Council of Canada and Solarchem Environmental Systems of Markham Ontario, Canada. We thank Dr. Stephen Cater, Dr. Ali Safarzadeh-Amiri, Mr. Keith Bircher, P. Eng, and Dr. R. D. Samuel Stevens of Solarchem Environmental Systems for their helpful comments and support during the conduct of this research.

Literature Cited

(1) Omura, K.; Matsuura, T. *Tetrahedron* **1968**, *24*, 3475.
(2) Ogata, Y.; Tomizawa, K.; Fujii, K. *Bull. Chem. Soc. Jpn.* **1978**, *51*, 2628.
(3) Bolton, J. R.; Cater, S. R. In *Aquatic and Surface Photochemistry*; Helz, G. R., Zepp, R. G., Crosby, D. G., Eds.; Lewis Publishers: Boca Raton, FL, 1994; pp 467−490.
(4) Leitzke, O.; Whitby, G. E. In *Proceedings: A Symposium on Advanced Oxidation Processes for the Treatment of Contaminated Water and Air*, June 4−5, 1990, Toronto ON, Canada.
(5) Weir, B. A.; Sundstrom, D. W.; Klei, H. E. *Hazard. Waste Hazard. Mater.* **1987**, *4*, 165.
(6) Sundstrom, D. W.; Weir, B. A.; Klei, H. G. *Environ. Prog.* **1989**, *8*, 6.
(7) Peyton, G. R.; Smith, M. A.; Peyton, B. M. *Photolytic Ozonation for Protection and Rehabilitation of Ground-Water Resources: A Mechanistic Study*; Report 87-206; University of Illinois Water Resources Center: 1987.
(8) Sundstrom, D. W.; Klei, H. E.; Nalette, T. A.; Reidy, D. J.; Weir, B. A. *Hazard. Waste Hazard. Mater.* **1986**, *3*, 101.
(9) Wolfrum, E. J. *A Kinetic Model of the H_2O_2/UV Process*; Symposium on Environmental Applications of Advanced Oxidation Techniques, EPRI & NSF, Feb 1993, San Francisco, CA.
(10) Glaze, W. H.; Lay, Y.; Kang, J. W. *Ind. Eng. Chem. Res.* **1995**, *34*, 2314.
(11) Frankenburg, P. E.; Noyes, W. A., Jr. *J. Am. Chem. Soc.* **1953**, *75*, 2847.
(12) Gardner, E. P.; Wijayaratne, R. D.; Calvert, J. G. *J. Phys. Chem.* **1984**, *88*, 5069.
(13) Nicholson, A. J. C. *Can. J. Chem.* **1983**, *61*, 1831.
(14) Dalton, J. C.; Turro, N. J. *Annu. Rev. Phys. Chem.* **1970**, *21*, 499.
(15) Berces, T. In *Comprehensive Chemical Kinetics*; Bamford C. H., Tripper, C. F., Eds.; Elsevier Publishing Co.: Amsterdam, The Netherlands, 1972; Vol. 5, p 309.
(16) Pieck, R.; Steacie, E. W. R. *Can. J. Chem.* **1955**, *33*, 1304.
(17) Noyes, W. A., Jr.; Porter, G.; Jolley, J. E. *Chem. Rev.* **1956**, *56*, 49.
(18) Volman, D. H.; Swanson, L. W. *J. Am. Chem. Soc.* **1960**, *82*, 4141.
(19) Anpo, M.; Kubokawa, Y. *Bull. Chem. Soc. Jpn.* **1977**, *50*, 1913.
(20) Qureshi, M.; Tahir, N. A. *J. Phys. Chem.* **1932**, *36*, 2670.
(21) The 200−300 nm photon flux was obtained from the total 200−500 nm photon flux by using the known spectral emission from the 1 kW Solarchem lamp. We calculated that 46% of the 200−500 nm photon flux lies in the 200−300 nm range.
(22) Murov, S. L.; Carmichael, I.; Hug, G. L. *Handbook of photochemistry*, 2nd ed.; Marcel Dekker Inc.: New York, 1993; p 299.
(23) Sutton, F. *A Systematic Handbook of Volumetric Analysis or The Quantitative Determination of Chemical Substances by measure, applied to liquids, solids and gases*, 13th ed.; Butterworths Scientific Publications: London, UK, 1955; p 307.
(24) Czapski, G.; Bielski, B. H. J. *J. Phys. Chem.* **1963**, *67*, 2180.
(25) Baxendale, J. H.; Wilson, J. A. *Trans. Faraday Soc.* **1957**, *53*, 344.
(26) Weeks, J. L.; Matheson, M. S. *J. Am. Chem. Soc.* **1956**, *78*, 1273.
(27) Hunt, J. P.; Taube, H. *J. Am. Chem. Soc.* **1952**, *74*, 5999.
(28) Dainton, F. S.; Rowbottom, J. *Trans. Faraday Soc.* **1953**, *49*, 1160.
(29) Buxton, G. V.; Greenstock, C. L.; Helman, W. P.; Ross, A. B. *J. Phys. Chem. Ref. Data* **1988**, *17*, 513.
(30) Bielski, B. H. J.; Cabelli, D. E.; Arudi, R. L.; Ross, A. B. *J. Phys. Chem. Ref. Data* **1985**, *14*, 1041.
(31) *Handbook of Chemistry and Physics*, 72nd ed.; Lide, D. R., Ed.; CRC Press Inc.: Boca-Raton, FL, 1991−1992; pp 8−39.

(32) Zegota, H.; Schuchmann, M. N.; Schulz, D.; von Sonntag, C. *Z. Naturforsch.* **1986**, *41B*, 1015.
(33) Adams, G. E.; Wilson, R. L. *Trans. Faraday Soc.* **1969**, *65*, 2981.
(34) Ogata, Y.; Tomizawa, K.; Takagi, K. *Can. J. Chem.* **1981**, *59*, 14
(35) Farhataziz, A.; Ross, A. B. *Natl. Stand. Ref. Data Ser.* (*U.S. Natl. Bur. Stand.*) **1977**, 59.
(36) Schuchmann, M. N.; Zegota, H.; von Sonntag, C. *Z. Naturforsch.* **1985**, *40 b*, 215.

Received for review November 16, 1995. Revised manuscript received February 12, 1996. Accepted February 19, 1996.[⊗]

ES950866I

[⊗] Abstract published in *Advance ACS Abstracts,* May 1, 1996.